Proceedings of International Conference on Heat Exchanger Fouling and Cleaning - 2011 (Peer-reviewed)
June 05 - 10, 2011, Crete Island, Greece
Editors: M.R. Malayeri, H. Müller-Steinhagen and A.P. Watkinson

Published online
www.heatexchanger-fouling.com

OPTICAL AND THERMAL INVESTIGATIONS OF CRYSTALLIZATION FOULING IN A MICRO HEAT EXCHANGER

M. Mayer[1], J. Bucko[2], W. Benzinger[3], R. Dittmeyer[4], W. Augustin[5] and S. Scholl[6]

[1 5 6] Technische Universität Braunschweig, Institute for Chemical and Thermal Process Engineering (ICTV),
Langer Kamp 7, 38106 Braunschweig, Germany
moriz.mayer@tu-braunschweig.de
[2 3 4] Karlsruhe Institute of Technology (KIT), Institute for Micro Process Engineering (IMVT)
Hermann-von-Helmholtz-Platz 1, 76344 Eggenstein-Leopoldshafen, Germany

ABSTRACT

Micro heat exchangers have particular advantages regarding heat and mass transfer such as intensive heat exchange, low material costs, high mass transfer rates and an excellent thermal efficiency. The sensitivity of micro structures to undesirable deposition is a fundamental knock-out criterion for many industrial applications. Crystallization fouling of inverse soluble salts on heat exchanger surfaces leads to an increase of the pressure drop, as far as total blocking of the micro channels. Furthermore fouling results in a reduction of the heat exchanger performance, in a maldistribution of flow in the micro structures and in a shorter residence time of the fluid. The intension of this work is the basic investigations of the fouling behavior in micro heat exchangers. Therefore fouling experiments with calcium carbonate ($CaCO_3$) in an experimental micro heat exchanger were carried out and observed with a digital microscope. The investigations included local temperature measurements confirmed by CFD simulation as well as the optical visualization of the fouling process inside the micro channels. The detected fouling resistances R_f were in the range of 10^{-5}-10^{-4} m^2 K W^{-1}. The fouling developed heterogeneously in the micro channels and in a number of runs the deposit built up a parabolic profile with less fouling at the inlet of the micro structure. Cleaning in place (CIP) was possible and also optically observed.

INTRODUCTION

Crystallization fouling on heat transfer surfaces can cause high damage to the heat exchanger as well as to the connected equipment (Epstein, 1983) (Müller-Steinhagen, 1999). It often raises considerable costs in construction and operation. The crystal deposition is usually formed by inverse soluble salts such as $CaCO_3$ and $CaSO_4 \cdot 2H_2O$ which crystallize heterogeneously on the hot heat exchanger surface (Bohnet, 1987). This process can be divided into heterogeneous nucleation, crystal growth, adhesion, removal and aging of the fouling (Bott, 1995). During nucleation and to some extend during crystal growth an interface between the crystal and the heat exchanger surface comes to existence (Mayer et al., 2011). Consequently the heat flux is reduced and the pressure drop increases. This results in a decline of the heat exchanger performance and an extensive cleaning task. Hence it is reasonable to formulate a fouling resistance (Eq. 1) from the heat balance. Figure 1 shows the fouling on a heat transfer surface schematically.

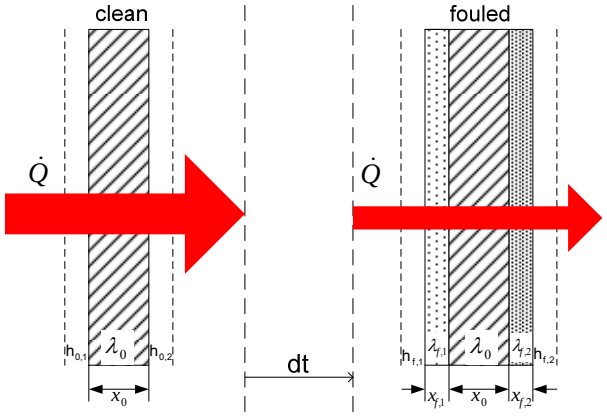

Fig. 1 Schematic diagram of the heat flux through a clean and a fouled heat exchanger wall.

$$R_f = \frac{1}{U_f} - \frac{1}{U_0} = \frac{1}{h_{f,1}} + \frac{x_{f,1}}{\lambda_{f,1}} - \frac{1}{h_{0,1}} + \frac{1}{h_{f,2}} + \frac{x_{f,2}}{\lambda_{f,2}} - \frac{1}{h_{0,2}} \quad (1)$$

Typical distributions of the fouling resistance are shown in Figure 2. At least two periods can be distinguished: The induction period, where the heat transfer is not reduced significantly, and the crystal growth period.
Many industrial heat exchangers are operated with a pH value above 7 in order to avoid corrosion. Unfortunately fouling rates rise with increasing pH value (Augustin et al., 1995). The driving power for crystallization fouling is the level of supersaturation at the heat exchanger surface which can be expressed by the saturation index SI (Eq. 2).

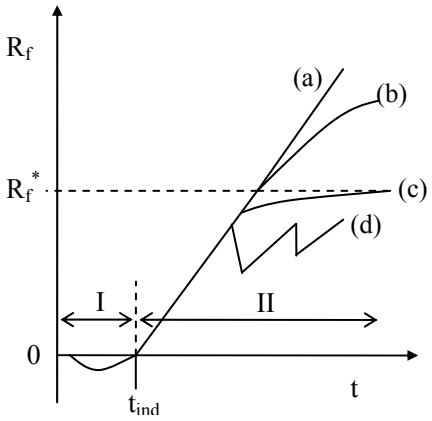

Fig. 2. Fouling resistance over time: I induction period, II layer growth period; (a) no removal, (b) decreasing deposition rate due to removal, (c) asymptotic behavior: deposition and removal rate become equal, (d) saw tooth shape: removal of bigger deposit fractions.

The saturation index is the common logarithm of the ratio of the actual ionic activity product to the solubility product. The solution at the wall must be supersaturated, i.e. the saturation index must be greater than zero for crystallization fouling (Mullin, 2005).

$$SI = \log\left(\frac{IAP}{K_{SP}}\right) = \log\left(\frac{\prod_1^i a_i}{\prod_1^i a_i^{eq}}\right) = \log\left(S(C, T_m)\right) \qquad (2)$$

Micro process engineering tries to adopt unit operations in a volume at micro scale. Typical micro heat exchangers are endowed with micro channels that have diameters of less than 1 mm. Due to the small dimensions micro heat exchangers are appropriate for processes with high heat and mass transfer rates. Hence they have advantages over conventional heat exchangers concerning the rate of product conversion, directed heating and short residence times (Schubert et al., 2001). However the usage in chemical industries is rare today since the micro structures are very vulnerable to corrosion and fouling. Therefore the contamination of micro heat exchangers and their cleaning needs to be studied. Figure 3 shows an example of a cross flow micro heat exchanger (Bucko et al., 2010).

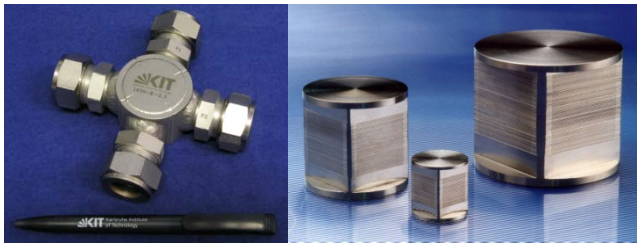

Fig. 3 Crossflow micro heat exchanger with a volume of 8 cm^3 (left) and micro structured cores for crossflow micro heat exchanger of different sizes (right).

MICRO HEAT EXCHANGER DESIGN

The experimental heat exchanger was constructed at the IMVT, KIT Karlsruhe. Figure 4 shows the experimental counter current micro heat exchanger for the fouling experiments (Mayer et al., 2010). The micro structured devices of the solution and the heating side as well as of the local temperature measuring points are shown in Figure 5 (Bucko et al., 2010).

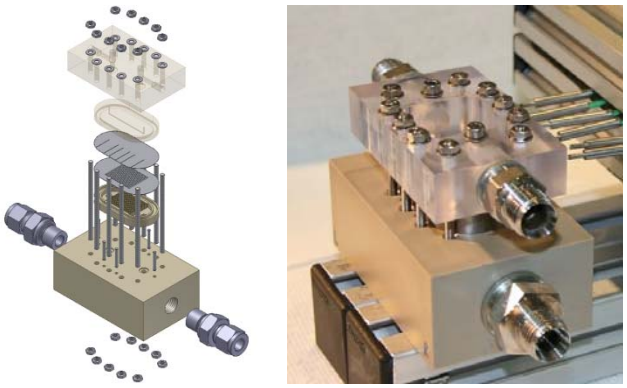

Fig. 4 Schematic exploded draft of the experimental micro heat exchanger (left) and assembled experimental micro heat exchanger for fouling investigation (right).

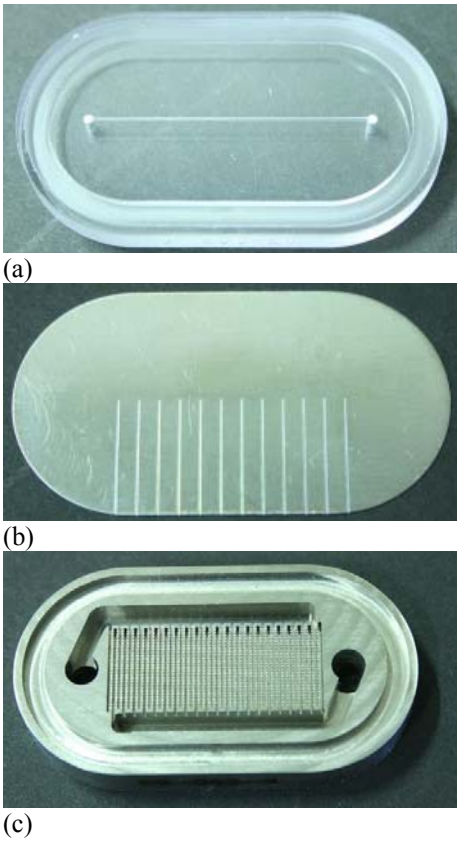

(a)

(b)

(c)

Fig. 5 Micro structured devices: (a) polycarbonate element with one micro channel, (b) heat transfer foil with 12 micro slots for thermocouples, (c) titan element for heating with 693 channels.

FOULING EXPERIMENTS

The upper test section is made from polycarbonate and thus transparent for the optical investigations. It is further removable for cleaning and for the insertion of different geometries. The investigated channels were rectangular with 400 µm width, 200 µm depth and 24 mm length. The corresponding structures had one, 12 respectively 18 channels. The heating device had 693 channels (200 x 200 x 600 μm^3) and provides nearly constant wall temperature on the heating side. Six respectively 12 thermocouples with a diameter of 150 µm were placed in micro slots with a cross section of 160 x 155 μm^2 between the two heat exchanger foils (each 200 µm thickness) centered in flow direction. All parts were clamped together with screws and sealed with Viton®.

Figure 6 shows the experimental setup. For the fouling experiments a supersaturated solution (25 °C) was pumped through the micro heat exchanger with a HPLC pump (Knaur, Smartline 100). The HPLC pump provided constant flow rate over the whole fouling experiment. In order to avoid fouling at the heating side distilled water was pumped counter current with 8 ml s^{-1}. Temperatures were measured at the inlet and outlet on both sides. The pressure was measured at the inlet and outlet of the solution side. In order to obtain the mean initial surface temperature T_m the temperatures from the six local measurement points were used.

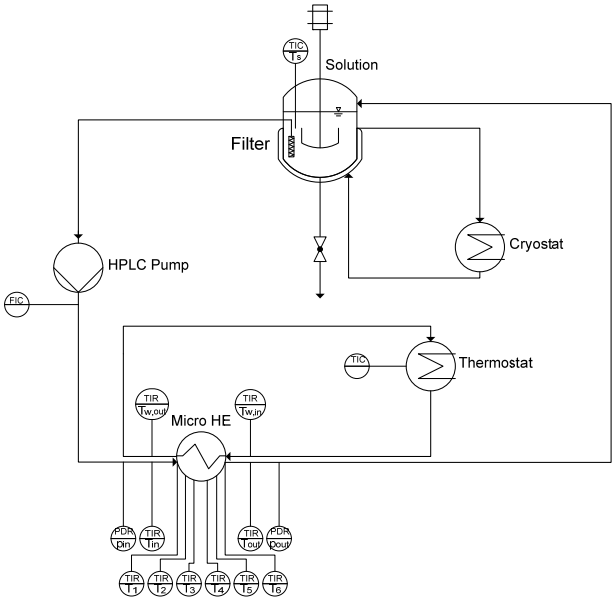

Fig. 6 Experimental setup.

The solution was aerated with CO_2 for 12 h in order to keep a high solubility of $CaCO_3$. Afterwards the solution was brought from about pH 5.3 to 7 with NaOH. The concentration of $CaCO_3$ was 5 mmol l^{-1} and the corresponding SI at the heat exchanger surface varied from 0.56 – 0.77. Flow rates were varied from 1 to 10 ml min^{-1} for one channel and from 10 to 40 ml min^{-1} for 12 channels respectively 18 channels. Under consideration of a uniform flow distribution at the inlet of the micro structures the corresponding Reynolds numbers Re were between 79 and 792 for one channel, between 66 and 264 for 12 channels and between 44 and 176 for 18 channels. To avoid damage to the micro structure the maximum pressure inside the HPLC pump was set to 3 MPa. After the fouling experiments the micro structures were cleaned by rinsing with 6% HCl solution for about 20 minutes and rinsing again for about 30 minutes with distilled water in order to remove the acid. The formation of the crystallization fouling was optically captured by a digital microscope (see Figure 7) (Keyence, VHX 500F) at different magnifications.

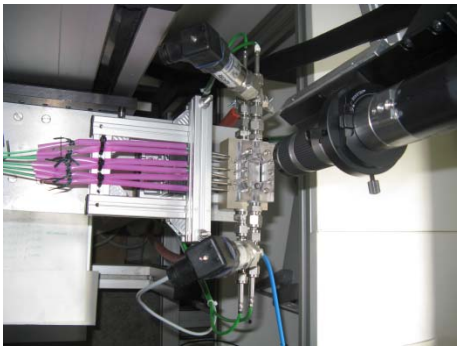

Fig. 7 Setup of micro heat exchanger with digital microscope at right (view from top).

RESULTS

In order to validate the temperature measurements CFD simulations (Ansys, Fluent 12.0) were carried out using the Navier-Stokes equations for incompressible fluids. The geometric model corresponding to the single channel micro structure (see Figure 5a) is shown in Figure 8.

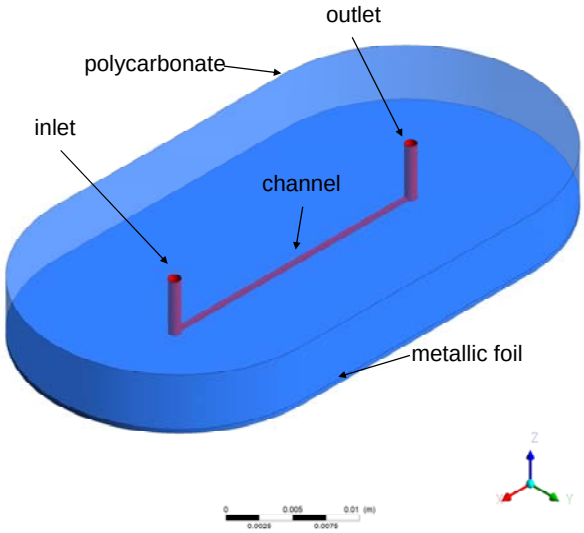

Fig. 8. Geometric model of the flow system: micro channel in polycarbonate with metallic bottom side.

The simulation was carried out with constant wall temperature and data for pure water at the same conditions as the experiments with different mass flows. Figure 9 shows a profile of the micro channel and the foil with micro slots for the thermocouples.

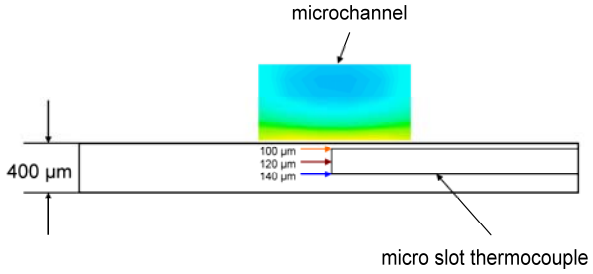

Fig. 9 Schematic profile for the micro channel and the metal foil with a micro slot. Arrows mark the possible measuring points of the thermocouple in the micro slots of the heat exchanger foil.

Figure 10 shows the experimental and simulation results of the local temperature measurements corresponding to Figure 9 for $2.1 \cdot 10^{-5}$ kg s^{-1} (1 ml min^{-1}) and for $1.4 \cdot 10^{-4}$ kg s^{-1} (8 ml min^{-1}). Due to the tetrahedral mesh used in the simulation small fluctuations of the simulated curves occurred. At higher flow rates the difference between the experimental and the calculated values increases. The experimental values were slightly higher than those obtained from the simulation. Figure 11 shows the experimental detected temperatures of the fluid and the temperatures from the simulation at the outlet of the micro structure. As a result from the heat balance the outlet temperature at the solution side sinks with increasing flow rate. The results are in good accordance for higher mass flow rates. An average standard deviation of 1.5 K was determined for the experimental results.

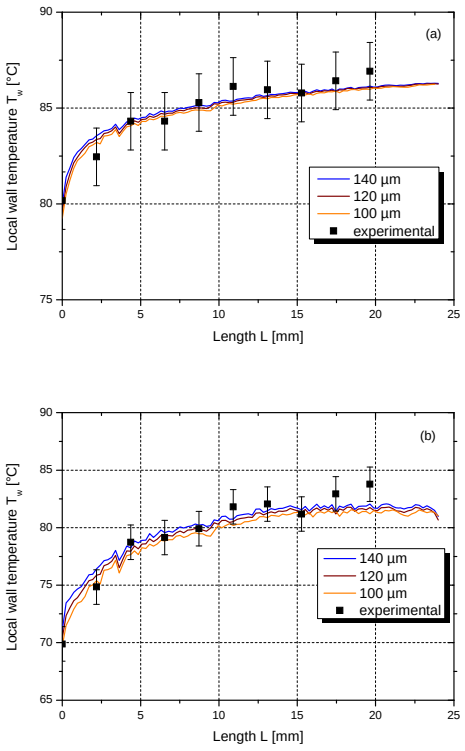

Fig. 10 Experimental vs. simulation results of the local temperature measurements: (a) $2.1 \cdot 10^{-5}$ kg s^{-1}, (b) $1.4 \cdot 10^{-4}$ kg s^{-1}.

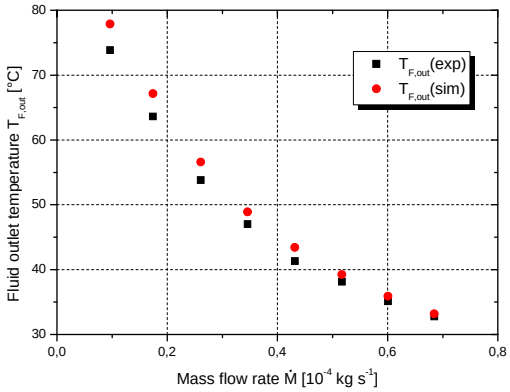

Fig. 11 Fluid temperature at the outlet versus the mass flow rate.

Typical examples for the optical detection of the fouling progress are shown in Figure 12. The crystal deposition appears dark in the pictures. In some cases a parabolic fouling layer was observed at the end of the experiment. This can be attributed to an uneven heat flux distribution inside the heating structure (Figure 4c). The corresponding integral fouling resistances from the heat balance are shown in Figure 13. The integral fouling resistance was calculated with Eq. (3) and the heat flux with Eq. (4).

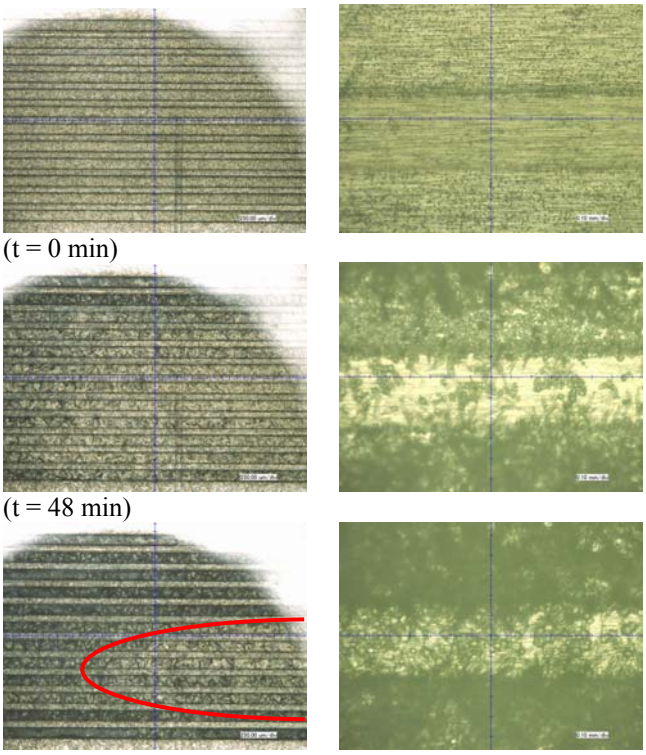

Fig. 12 $CaCO_3$ in micro structures over time (flow from right to left, crystals appear dark). Left column: 12 channels (40 ml min^{-1}; T_m = 60 °C; 30x magnified, parabolic fouling

profile at the end. Right column: single channel (10 ml min^{-1}; T_m = 80 °C; 200x magnified).

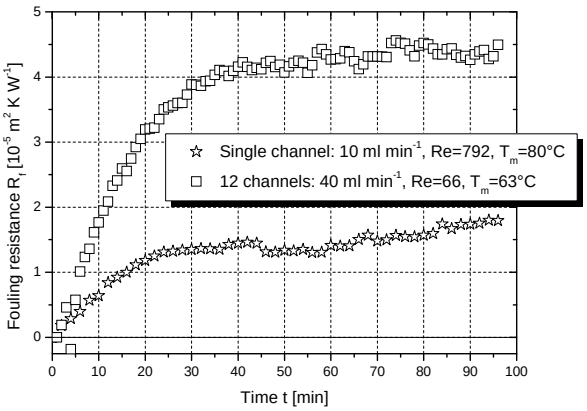

Fig. 13 Fouling resistances corresponding to Figure 12.

$$R_f(t) = \frac{A \cdot \Delta T_{log,f}(t)}{\dot{Q}_f(t)} - \frac{A \cdot \Delta T_{log,0}}{\dot{Q}_0} \quad (3)$$

$$\dot{Q}(t) = \dot{M}(t) \cdot c_p(t) \cdot \left(T_{out}(t) - T_{in}\right) \quad (4)$$

In Eq. (3) the heat transfer area of the micro channels A was assumed to be constant since the crystal deposition acts as an insulator for the conductive heat transfer. In Eq. (4) only the outlet temperature changed significantly over time; the mean mass flow rate and the mean heat capacity of the solution changed hardly while the volume flow rate and the inlet temperature were kept constant.

The cleaning in place (CIP) was also detected with the digital microscope. Figure 14 shows the cleaning of the $CaCO_3$ fouled 18 micro structure channels with a 6% HCl solution at different times.

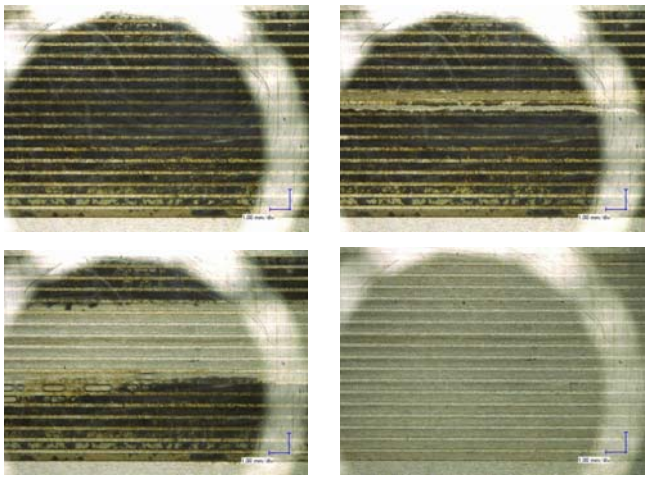

Fig. 14 CIP (HCl 6 wt-%) of a 18 micro structure chanels fouled with $CaCO_3$; from top left to bottom right (0 min; 10.5 min; 16.5 min; 18.5 min) 20x magnified, flow from right to left.

DISCUSSION

It was shown that it is possible to measure the local temperature inside the heat exchanger foil of a micro heat exchanger through micro slots. The obtained values are in good accordance with the results of the CFD simulation. The initial mean surface temperature T_m and the corresponding saturation index SI could be determined with the local temperature measurements. During the fouling progress the local temperature showed an inhomogeneous distribution due to the cross conduction inside the heat exchanger foil. This made it difficult to summarize the local fouling resistances. In the future the fouling process itself needs to be modeled and simulated through a mass and a heat balance.

The pictures taken with the digital microscope showed the fouling inside the micro structure. It was observed that the fouling occurred also below the ligaments between the channels. This can be attributed to the fact that the micro channels were not sealed. Furthermore the optical investigations showed a maldistribution for the 12 channel micro structure caused by fouling with a parabolic fouling layer for longer periods that can be attributed to an uneven heat flux distribution in the heating structure (see Figure 12). The optically detected fouling density (see Figure 12) is not directly comparable to the fouling resistance from the integral heat balance (see Figure 13) because there was a high heat transfer in the inlet and outlet distributors of the micro structures (see Figure 5 (a)) which cannot be neglected. The integral fouling resistance showed an asymptotic behavior with very short induction periods (see Figure 13). The asymptotic behavior can be explained through a decreasing saturation index (Eq. 1) due to a decreasing surface temperature. When fouling occurs also the influence of an increasing pressure drop needs to be taken into consideration. There was no removal detected neither through temperature measurements nor through optical capture (Mayer et al., 2010). In comparison to an industrial sized heat exchanger the flow velocities and the according wall shear stresses in the investigated micro heat exchangers are high but the flow regime is laminar (Re < 2300). It is possible that a flow induced removal on microscale depends mainly on the degree of turbulence rather than on wall shear stress. Since the observed crystallization fouling is reaction controlled the effect of the mass transfer has been not considered yet. Also the deposit thickness could not be measured. The CIP with acid was enhanced by possible bypass flows below the ligaments of the micro channels due to the clamped construction of the micro heat exchanger. Once a number of the channels were free the cleaning rate increased (see Figure 9). A measure to reduce the adhesion could be a surface treatment. Investigations of the adhesion of crystals on heat exchanger surfaces showed a significant reduction of $CaCO_3$ fouling on surfaces modified with diamond-like-carbon based coatings (Mayer et al., 2011). An additional surface layer or coating on the heat exchanger foil would not decrease the channel diameter nor increase the pressure drop due to the clamped construction. Only the additional thermal resistance of the coating must be considered. For a standard DLC coating with thickness of 3 µm this is negligible. It

could be also helpful to use electro polished heat exchanger surfaces in micro process engineering in order to enhance the CIP.

CONCLUSIONS

1. It could be pointed out that crystallization fouling of $CaCO_3$ at a relatively high supersaturation level has a significant and fast impact on the degradation of the performance of the micro heat exchanger. The measurement of local wall temperatures was possible and was in good agreement with CFD simulations. Through the experimental heat exchanger with optical accessible micro channels the fouling progress and its cleaning was observed. The fouling resistance was determined from an integral heat balance. The cross conduction inside the heat transfer foil has not been considered yet.
2. The obtained results could be applied at the construction of micro heat exchangers. In general a similar fouling behavior like in macroscale heat exchangers was observed. Since crystallization fouling causes high damage to the micro structured system it is either crucial to avoid fouling through closed systems or to construct a micro heat exchanger that bears a certain amount of unwanted deposit and can be cleaned easily. The influence of the pressure drop in fouling in micro structures needs to be investigated. Further studies should concentrate on the usage of modified surfaces in micro heat exchangers and cleaning possibilities. It was demonstrated that in principle crystallization fouling in micro structures can be removed by applying HCl and acid-resistant surfaces. The design of micro structures must avoid a maldistribution of the flow if fouling occurs. Since the impact of crystallization fouling depends strongly on the flow velocity and surface temperature flow dead zones particularly in the distributors need to be avoided. Flow dead zones can be prevented through small inlet and outlet distributors which should be also at microscale. Also gauging accesses to the micro structures for example for pressure sensors can have a negative effect. The optical results could be applied to time schedules for CIP of micro structures that do not have optical accessibility.

NOMENCLATURE

A	heat transfer area, m^2
a	activity, dimensionless
C	concentration, mol m^{-3}
c_p	heat capacity, kJ kg^{-1} K^{-1}
h	heat transfer coefficient, W m^{-2} K^{-1}
IAP	ionic activity product, dimensionless
K_{sp}	equilibrium solubility product, dimensionless
L	length, m
$\dot{M}$	mass flow rate, kg s^{-1}
$\dot{Q}$	heat duty, W
R_f	fouling resistance, m^2 K W^{-1}
Re	Reynolds number, dimensionless
S	supersaturation, dimensionless
SI	saturation index, dimensionless
$T_{F,out}$	fluid outlet temperature, K
T_m	initial mean surface temperature, K
T_w	wall temperature, K
t	Time, s
U	overall heat transfer coefficient, W m^{-2} K^{-1}
x	thickness, m
λ	thermal conductivity, W m^{-1} K^{-1}
ΔT_{log}	logarithmic mean temperature difference, K

Subscript

eq	equilibrium
f	fouled
i	encounter
ind	induction
0	clean
1,2	sides

REFERENCES

Augustin, W. and Bohnet, M., 1995, Influence of the ratio of free hydrogen ions on crystallization fouling, *Chem. Eng. Process.*, Vol. 34, pp. 79-85.

Bohnet, M., (1987), Fouling of Heat Transfer Surfaces, *Chem. Eng. Technol*., Vol. 10, pp. 113 – 125.

Bott, T., 1995, *Fouling of heat exchangers*, Elsevier.

Bucko, J., Benzinger, W., Mayer, M., Augustin, W., Scholl, S., Dittmeyer, R., 2010, Experimental and CFD Results for Local Temperature Measurement in Microstructure Devices, *Proceedings 2nd µFluidic Conference - 2010*, Toulouse, France.

Epstein, N., 1983, Thinking about heat transfer fouling: A 5 x 5 matrix, *Heat Trans. Eng.*, Vol. 4, pp. 43-56.

Mayer, M., Augustin, W. and Scholl, S., 2011, Experimental study on the adhesion of single crystals on modified surfaces in crystallization fouling, *Proceedings of the International Conference on Heat Exchanger Fouling and Cleaning IX – 2011*, Crete, Greece.

Mayer, M., Bucko, J., Benzinger, W., Dittmeyer, R., Augustin, W. and Scholl S., 2010, Investigation and Visualization of crystallization fouling in a micro heat exchanger, *Proceedings of the 2nd European Conference on Microfluidics - 2010,* Toulouse, France.

Mullin, J., 2005, *Crystallization and Precipitation*, Wiley-VCH, Weinheim, Germany.

Müller-Steinhagen, H., 1999, Cooling-water fouling in heat exchangers, *Adv. Heat Trans.*, Vol. 33, pp. 415-496.

Schubert, K., Brandner, J.J., Fichtner, M., Lindner, G., Schygulla, U., Wenka, A., 2001, Microstructure Devices for Applications in Thermal and Chemical process Engineering, *Microscale Thermophys. Eng*, Vol. 5, pp. 17-39.